Inorganic Chemistry

Communication

pubs.acs.org/IC

Structural Assembly from Phosphate to Germanophosphate by Applying Germanate as a Binder

Ya-Xi Huang,*[,†] Biao Liu,[†] Lei Wen,[†] Xin Zhang,[†] Wei Sun,[†] Jun Lin,[‡] Chun-Zuo Huang,[†] Rong-Chuan Zhuang,[§] Jin-Xiao Mi,[†] and Jing-Tai Zhao[∥]

[†]Department of Materials Science and Engineering, College of Materials, Xiamen University, Xiamen 361005, China

[∥]State Key Laboratory of High Performance Ceramics and Superfine Microstructure, Shanghai Institute of Ceramics, Chinese Academy of Science, Shanghai 200050, China

[‡]Key Laboratory of Nuclear Analysis Techniques, Shanghai Institute of Applied Physics, Chinese Academy of Sciences, Shanghai 201800, China

[§]Xiamen Zijin Mining and Metallurgy Technology Co. Ltd., Xiamen 361101, China

Supporting Information

ABSTRACT: Structural assembly from phosphate to germanophosphate by applying germanate as a binder has been achieved. Two isotypic porous compounds, $K_3[M^{II}_4(HPO_4)_2][Ge_2O(OH)(PO_4)_4]\cdot xH_2O$ (M^{II} = Fe, Cd; x = 2 for Fe and 3 for Cd, denoted as **KFeGePO-1** and **KCdGePO-1**, respectively), contain a known transition-metal phosphate (TMPO) layer, $^2_\infty\{[M_2(HPO_4)_3]^{2-}\}$, which is built from chains of trans-edge-sharing MO_6 octahedra bridged by MO_5 trigonal bipyramids that were further linked and decorated by phosphate tetrahedra. The layers are bound by infinite chains of $GeO_5(OH)$ octahedra, resulting in a 3D open-framework structure with 1D 12-ring channels that are occupied by K^+ ions and water molecules. The curvature of the TMPO layers and shape of the 12-ring windows can be tuned by the transition metals because of their Jahn–Teller effect.

Germanates have been approved to have extra-large pores in their structure and may have promising application as candidates to replace silicates in gas absorbents, catalysts, and separators in the chemical and petroleum industries.[1] Incorporating heteroatoms into germanate frameworks increases the structural diversity and generates another class of materials with interesting structures and properties.[2] Transition metals and rare earths, containing a d- or f-shell electron, are candidates to obtain compounds with interesting physical properties, such as optical, magnetic, and electric properties.[3] However, it is a great challenge to directly obtain transition-metal germanates without applying organic ligands or coordinated groups. To our knowledge, phosphate has a strong affinity to transition metals.[4] On the basis of this feature, one can expect to fuse transition metals to germanates by adding phosphate, which may be able to overcome the obstacle and become a heteroanionic system for gaining considerable structural diversity and useful physical properties.

The resulting heteroanionic system is germanophosphate (GePO), which is a quite young subject with regard to germanates. Many features of GePOs are still waiting to be discovered. To date, most of the known GePOs have been prepared by conventional solid-state reactions at high temperatures, which lead to dense structures.[5] By use of a hydro/solvothermal method, several transition-metal GePOs have been synthesized.[6] Very recently, we obtained a series of transition-metal GePO compounds,[7] whose structures consist of zigzag metal octahedral chains linked by germanium phosphate pentamers. However, these previously reported transition-metal GePOs, except the zinc compound,[6a] did not exhibit expected porous features. During our investigations on porous GePOs, by applying alkali metal as the template, we successfully obtained two isotypic porous compounds, **KFeGePO-1** and **KCdGePO-1**, containing 12-ring channels. In the structure, a known transition-metal phosphate layer was bound by germanate chains to a porous framework structure.

KFeGePO-1 and **KCdGePO-1** have been solvothermally synthesized. For **KFeGePO-1**, a mixture with a molar ratio of GeO_2/Fe/KCl/H_3PO_4/H_2O/1,2-propanediol/triethylamine = 0.7:0.25:2:14.6:111:21:14.4 was transferred into a Teflon-lined stainless-steel autoclave (15 mL in volume) and heated at 190 °C for 5 days under static conditions. A similar process was applied for **KCdGePO-1**, but $Cd(AC)_2\cdot 2H_2O$ (0.266 g, 1 mmol) takes the place of iron powder. Colorless prismatic crystals in high yield (about 80%, based on Fe/Cd) were obtained. The phase purities of two compounds have been checked by performing powder X-ray diffraction (PXRD). Qualitative energy-dispersive X-ray analysis results confirmed the presence of K, Ge, Fe/Cd, and P (Figure S1 in the Supporting Information, SI). IR spectra confirmed the presence of a hydroxyl (OH) group and water molecules (Figure S2 in the SI). Thermal analysis results of **KFeGePO-1** showed a two-step weight loss with a total amount of 5.6%, which agrees well with the removal of two water molecules and the condensation of three OH groups (calcd 5.6%; Figure S3a in the SI). For **KCdGePO-1**, a similar thermal decomposition process has been taken: because of its one additional channel water, the total weight loss is about 5.7% (calcd 5.9%, for the removal of three water molecules and three OH groups). The divalent state of Fe^{2+} was confirmed by

Received: May 30, 2013
Published: August 8, 2013

dx.doi.org/10.1021/ic401329d | *Inorg. Chem.* 2013, 52, 9169–9171

Mössbauer spectrometry (Figure S4 in the SI). Magnetic susceptibility results reveal that **KFeGePO-1** exhibits antiferromagnetic properties at lower temperatures (Figure S5 in the SI).

KFeGePO-1 and **KCdGePO-1**[9] (Figure 1) have similar framework structures but differ in the channel shape and channel species arrangement. Here we choose the iron compound as an example to illustrate the conformation of their frameworks. In **KFeGePO-1**, the crystal structure is built from FeO_6 octahedra, FeO_5 trigonal bipyramids, $GeO_5(OH)$ octahedra, and HPO_4 and PO_4 tetrahedra. The framework contains two orientation-different ferrous ribbons, built from chains of trans-edge-sharing FeO_6 octahedra running along [001] loop-branched by FeO_5 trigonal bipyramids in an up-and-down manner alternately, which are stacked along [010] in an "ABAB" fashion (Figure 1a). The resulting ribbons are further interconnected by HPO_4 groups to form an undulated layer parallel to the *bc* plane, with additional PO_4 tetrahedra decorating either side (Figure 1b). Such ferrous phosphate layers are linked by infinite chains of trans-corner-sharing $GeO_5(OH)$ octahedra, resulting in a 3D framework structure with 1D 12-ring channels parallel to the *c* axis in which K^+ ions and water molecules reside (Figure 1c). The inorganic framework can maintain after removal of the channel water, as indicated by in situ PXRD (Figure S3b in the SI).

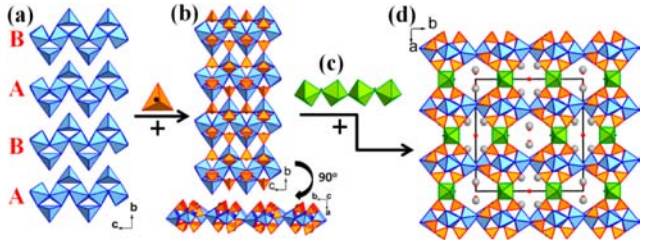

Figure 1. Framework conformation of **KFeGePO-1**: (a) Two differently oriented ferrous ribbons, built from chains of trans-edge-sharing FeO_6 octahedra bridged by FeO_5 trigonal bipyramids, stacked along [010] in an "ABAB" fashion. (b) The successive ribbons are stapled by HPO_4 tetrahedra and decorated by PO_4 groups on either side to form a layer. (c) A $GeO_5(OH)$ octahedral single chain is shown. (d) The layers are bound by germanate chains to result in a 3D framework with 1D 12-ring channels running along [001] in which K^+ ions and water molecules reside. Color code: FeO_6/FeO_5 polyhedra, blue; $GeO_5(OH)$ octahedra, green; PO_4 tetrahedra, orange; K atoms, medium-gray balls; O atoms, red balls; H atoms, dark-gray balls.

It is worth noting that the transition-metal phosphate (TMPO) layer has been found in a layered manganese phosphate $(C_2H_{10}N_2)[Mn_2(HPO_4)_3(H_2O)]$ (see Figure 2a).[8] There the MnPO layer has the same conformation as that of the title compounds; the interlayer spaces are filled with ethylenediaminium ions and water molecules, which interlink the MnPO layers via hydrogen bonds. For the title compounds, the successive TMPO layers are clutched tightly by $GeO_5(OH)$ octahedral chains via common oxygen vertices, with four neighboring PO_4 groups leading to a relatively flexible 3D framework. That is to say, the 3D framework can be treated as a structural assembly from 2D TMPO layers by applying $GeO_5(OH)$ octahedral chains as binders (see Figure 2).

As shown in Figure 2, flat CdPO layers are observed in **KCdGePO-1**, whereas undulating FePO layers are found in **KFeGePO-1**. Because of the different curvature of TMPO layers, two almost equal pseudohexagonally shaped 12-ring channels

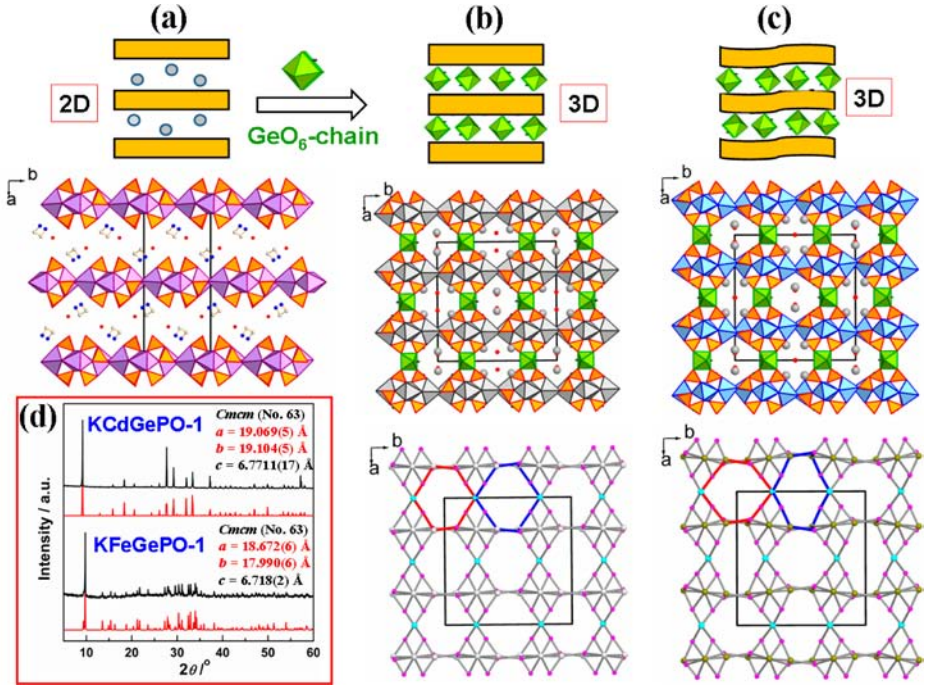

Figure 2. Top: Schematic presentation for the structural assembly from a 2D layer to a 3D framework by applying GeO_6 single chains as binders. Middle: (a) layered structure of $(C_2H_{10}N_2)[Mn_2(HPO_4)_3(H_2O)]$,[8] (b) flat layers bound by GeO_6 chains in **KCdGePO-1**, and (c) undulated layers bound by GeO_6 chains in **KFeGePO-1**. Bottom: topological presentation of **KCdGePO-1** (b) and **KFeGePO-1** (c) clearly showing the different shapes of the 12-ring channels (outlined with blue and red lines). (d) Experimental (black) and calculated (red) PXRD patterns of **KCdGePO-1** and **KFeGePO-1**, with Cu Kα radiation. Color code: MnO_x polyhedra, purple; CdO_x polyhedra, light gray; FeO_x polyhedra, blue; $GeO_5(OH)$ octahedra, green; PO_4 tetrahedra, orange; K atoms, medium-gray balls; O atoms, red balls; H atoms, dark-gray balls; C atoms, light-gray balls; N atoms, blue balls; Fe atoms, yellow-green balls; Cd atoms, light-gray balls; Ge atoms, turquoise balls; P atoms, purple balls.

dx.doi.org/10.1021/ic401329d | *Inorg. Chem.* 2013, 52, 9169−9171

with aperture sizes of 9.31 × 7.38 and 9.76 × 7.60 Å were formed in the cadmium compound, while an elongated channel (10.48 × 5.65 Å) and a regular hexagonally shaped channel (8.20 × 8.12 Å) are found for **KFeGePO-1**. Because of distortion of the channels, the Ow1 atom in the cadmium compound is assigned as full occupancy, while half-occupancy occurs in the iron compound.

The structure difference between **KCdGePO-1** and **KFeGePO-1** can be easily detected from their PXRD patterns. **KFeGePO-1** has more reflections than **KCdGePO-1**, although both of them crystallize in the same orthorhombic space group, *Cmcm* (see Figure 2d). The difference between them may lie in the undulated degree of the TMPO layer, or even may be due to the Jahn−Teller effect of transition metals, as well as the channel species arrangement constrained by the channel shape. According to crystal-field theory, Cd^{2+} is a d^{10} ion, its electron density in the T_{2g} and E_g orbitals has O_h symmetry, and thus it has no Janh−Teller effect. However, for high-spin Fe^{2+} (d^6), the electronic state is not spatially symmetric; thus, E_g will spatially degenerate to lower the energy.[10] As a result, the bond distances of Fe−O vary in a larger range than those of Cd−O [magnitude of bond distortion (d_{max}/d_{min}): 1.11 and 1.03 for $Fe1O_6$ and $Cd1O_6$ octahedron, respectively; 1.18 and 1.11 for $Fe2O_5$ and $Cd2O_5$ trigonal bipyramid, respectively]. The maximum torsion angle of Fe1−O6−Fe1 [104.0(2)°] is much larger than that of Cd1−O6−Cd1 [97.10(18)°] as well. The larger torsion angle of the iron compound makes its TMPO layers more undulating than that of the cadmium compound. It is worth noting that the different curvature of the TMPO layers also gives a hint of the structural flexibility.

In summary, the structural assembly from phosphate to GePO by applying germanate as a binder has been achieved. It is the first time to observe that a known 2D transition-metal phosphate layer {layers in $(C_2H_{10}N_2)[Mn_2(HPO_4)_3(H_2O)]$} can be bound by germanate units to form a 3D framework structure. The Jahn−Teller effect makes the iron compound have undulated layers while the cadmium compound has flat layers, which further results in different shapes of 12-ring channels and quite different PXRD patterns. Furthermore, the different curvatures of TMPO layers and channel shapes also give a hint of the structural flexibility. We suppose that Cu ions, having the strongest Jahn−Teller effect, may be able to be introduced into the structure. These kinds of structural assembly strategies may open a new vista for the design of new GePOs with diverse structures and interesting properties.

■ ASSOCIATED CONTENT

Supporting Information

SEM images, FTIR spectra, TGA curves, in situ PXRD, Mössbauer spectra, magnetic properties, table of selected bond distances and angles, and crystallographic information files in CIF format. This material is available free of charge via the Internet at http://pubs.acs.org.

■ AUTHOR INFORMATION

Corresponding Author

*E-mail: yaxihuang@xmu.edu.cn.

Notes

The authors declare no competing financial interest.

■ ACKNOWLEDGMENTS

This work was supported by the National Natural Science Foundation of China (Grants 21201144, 21233004, and 40972035), the Fundamental Research Funds for the Central Universities (Grant 2013121020), and the Technological Innovation Platform of Fujian Province (Grant 2006L2003). We appreciate Prof. Dr. Gen-Fu Chen for his magnetic measurements and suggestions, as well as Lei Shi for his Brunauer−Emmett−Teller measurements and discussions.

■ REFERENCES

(1) (a) O'Keeffe, M.; Yaghi, O. *Chem.—Eur. J.* **1999**, *5*, 2796−2801. (b) Zou, X. D.; Conradsson, T.; Klingstedt, M.; Dadachov, M. S.; O'Keeffe, M. *Nature* **2005**, *437*, 716−719. (c) Lin, Z.-E.; Yang, G.-Y. *Eur. J. Inorg. Chem.* **2010**, 2895−2902.

(2) (a) Nguyen, Q. B.; Lii, K. H. *Inorg. Chem.* **2012**, *51*, 9150−9152. (b) Dadachov, M. S.; Sun, K.; Conradsson, T.; Zou, X. D. *Angew. Chem., Int. Ed.* **2000**, *39*, 3674−3676. (c) Francis, R. J.; Jacobson, A. J. *Angew. Chem., Int. Ed.* **2001**, *40*, 2879−2881.

(3) (a) Wang, X.; Wang, Y.; Liu, Q.; Li, Y.; Yu, J.; Xu, R. *Inorg. Chem.* **2012**, *51*, 4779−4783. (b) He, H.; Cao, G. J.; Zheng, S. T.; Yang, G. Y. *J. Am. Chem. Soc.* **2009**, *131*, 15588−15589.

(4) Natarajan, S.; Mandal, S. *Angew. Chem., Int. Ed.* **2008**, *47*, 4798−4828.

(5) (a) Alami, M.; Brochu, R.; Soubeyroux, J. L.; Gravereau, P.; Flem, G. L.; Hagenmuller, P. *J. Solid State Chem.* **1991**, *90*, 185−193. (b) Zhao, D.; Xie, Z.; Hu, J.-M.; Zhang, H.; Zhang, W.-L.; Yang, S.-L.; Cheng, W.-D. *J. Mol. Struct.* **2009**, *922*, 127−134. (c) Brochu, R.; Loueer, M.; Alami, M.; Alquraoui, M.; Loueer, D. *Mater. Res. Bull.* **1997**, *32*, 113−122. (d) Winand, J.-M.; Rulmont, A.; Tarte, P. *J. Solid State Chem.* **1993**, *107*, 356−361. (e) Engel, G.; Fischer, U. *Z. Kristallogr.* **1985**, *173*, 101−112. (f) Popa, K.; Wallez, G.; Bregiroux, D.; Loiseau, P. *J. Solid State Chem.* **2011**, *184*, 2629−2634.

(6) (a) Li, J. M.; Ke, Y. X.; Zhang, Y. G.; He, G. F.; Jiang, Z.; Nishiura, M.; Imamoto, T. *J. Am. Chem. Soc.* **2000**, *122*, 6110−6111. (b) Liu, Y.; Yang, X.-L.; Zhang, J.; Li, Y.-Z.; Song, Y.; Du, H.-B.; You, X.-Z. *Chem. Commun.* **2008**, 3145−3147. (c) Liu, Y.; Yang, X.-L.; Wang, G.-L.; Zhang, J.; Li, Y.-Z.; Du, H.-B.; You, X.-Z. *J. Solid State Chem.* **2008**, *181*, 2542−2546.

(7) (a) Huang, Y.-X.; Zhang, X.; Huang, X.; Schnelle, W.; Lin, J.; Mi, J.-X.; Tang, M.-B.; Zhao, J.-T. *Inorg. Chem.* **2012**, *51*, 3316−3323. (b) Zhang, X.; Wen, L.; Chen, H.-M.; Mi, J.-X.; Huang, Y.-X. *Acta Crystallogr., Sect. E: Struct. Rep. Online* **2012**, *68*, i37−i38.

(8) Escobal, J.; Pizarro, J. L.; José, L.; Lezama, L.; Olazcuaga, R.; Arriortua, M. I.; Rojo, T. *Chem. Mater.* **2000**, *12*, 376−382.

(9) The crystal structures were solved and refined by using the *SHELX* programs (Sheldrick, G. M. *Acta Crystallogr.* **2008**, *A64*, 112−122). Crystal data: orthorhombic, *Cmcm* (No. 63), at 173 K. **KFeGePO-1**: a = 18.672(6) Å, b = 17.990(6) Å, c = 6.718(2) Å, V = 2256.6(12) Å^3, Z = 4; D_{calc} = 3.316 g·cm^{-3}; 130 free parameters; GOF = 1.158; $R1$ = 0.0486 [$I > 2\sigma(I)$], $wR2$ = 0.0996 for all data; residual electron density (max/min) = 1.203/−1.133 e·Å^{-3}. **KCdGePO-1**: a = 19.069(5) Å, b = 19.104(5) Å, c = 6.7711(17) Å, V = 2466.7(11) Å^3, Z = 4; D_{calc} = 3.692 g·cm^{-3}, 126 free parameters; GOF = 1.078, $R1$ = 0.0377 [$I > 2\sigma(I)$], $wR2$ = 0.0994 for all data; residual electron density (max/min) = 2.713/−1.037 e·Å^{-3}. Detailed information may be found on the ICSD (see CSD-426507 and CSD-426506 for **KFeGePO-1** and **KCdGePO-1**, respectively).

(10) Bersuker, I. *The Jahn−Teller Effect*; Cambridge University Press: Cambridge, U.K., 2006.